CHEMICAL ENGINEERING TRANSACTIONS
VOL. 80, 2020
A publication of AIDIC
The Italian Association of Chemical Engineering
Online at www.cetjournal.it
Guest Editors: Eliseo Maria Ranzi, Rubens Maciel Filho

ISBN 978-88-95608-78-5; **ISSN** 2283-9216
DOI: 10.3303/CET2080036

Pyrolysis of Humins Obtained from Acid-catalyzed Depolymerization of Rice Husk Cellulose: Model-Free Approach to Non-Isothermal Kinetics

Alana P. Gomes[a], Gabriel B. Salles[b], Marina G. Macedo[a], Paula G. A. Gonzalez[a], Yurany C. Ardila[c], Jaiver E. Jaimes Figueroa[d], Viktor O. C. Concha[a], Laura P. Tovar[a,*]

[a]Chemical Engineering Department, Federal University of São Paulo, 09972-270, Diadema, SP, Brazil
[b]Chemical Engineering Department, Federal University of Santa Maria, 97105-900, Santa Maria, RS, Brazil
[c]Universidad Industrial de Santander, Barbosa, Santander, Colombia
[d]Chemical Engineering Department, Federal University of Maranhão, 65080-805, São Luis, MA, Brazil
laura.tovar@unifesp.com

Humins (HUs) are one of the main by-products during levulinic acid production. In this work, HUs obtained from rice husk biorefining were investigated. The pyrolysis process in non-isothermal conditions (from 15°C to 900°C) using thermal analyses (TGA) was investigated. The HUs decomposition/pyrolysis process revealed a mass-loss between 65 and 93% depending on the variation of the heating rate. The loss of mass was attributed to the vaporization of water, followed by two main stages such as active (in two peaks) and passive pyrolysis. The Kissinger model-free method was applied to calculate kinetic parameters, estimating E_α of 97.8 kJ·mol^{-1} (for active pyrolysis – peak 1) and 260.2 kJ·mol^{-1} (for active pyrolysis – peak 2), respectively. The thermodynamic parameters (ΔH, ΔS, and ΔG) were calculated for active pyrolysis region. The values of ΔH were positives, indicating that the reaction is endothermic. Evaluating spontaneity of the reaction, positive ΔG and negative ΔS values characterize a non-spontaneous process. Therefore, these encouraging results lead to the HUs valorization in new concepts of biorefinery.

1. Introduction

Nowadays, every subject related to green chemistry, sustainability, bio-products and others has significant relevance and draws attention, and because of this the development of those new values found in the bio-economics model occurs. Latin America, for instance, is constantly looking for bio-economic solutions, even though it is a region rich in fossil and mineral raw materials, also known as non-renewable (Sasson and Malpica, 2018). In this scenario, humins are emerging as a potential material for the production of synthesis gas and commodities from pyrolysis processes.Humins (HUs) are byproducts of the process of obtaining hydroxymethylfurfural (5-HMF) and levulinic acid (LA) through C-6 sugar dehydration (Agarwal et al., 2017, Leal Silva et al., 2018). They have a variety of components, among them are mostly aliphatic hydrocarbons, in smaller amount carbohydrates, peptidoglycans and peptides and, finally, as a minority, lignin-derived components (Hayes et al., 2017). A relevant amount of carbohydrate raw materials, of approximately 30% in mass, may degrade to HUs, causing the reduction of the economic efficiency of biorefineries (van Zandvoort et al., 2015).Therefore, recently, HUs have been increasingly studied, so that the knowledge about this byproduct helps the viability of these industries. Besides, HUs are of paramount importance because they are powerful sources of heat and energy when they undergo the process of pyrolysis or gasification (van Zandvoort et al., 2015).Because they still are a byproduct little studied and of low knowledge regarding their structure and properties, the acknowledgment of HUs is still sparse. In open literature, information regarding the kinetics of thermal/pyrolysis decomposition is scarce, because researchers reporting the thermogravimetric analyzes and the thermal behavior do not determine the kinetic decomposition parameters. However, HUs have great potential due to their elemental composition. The value of HUs in the sphere of bio-

Paper Received: 28 November 2019; Revised: 17 February 2020; Accepted: 4 April 2020
Please cite this article as: Gomes A.P., Salles G.B., Macedo M.G., Gonzalez P.G.A., Ardila Y.C., Jaimes Figueroa J.E., Concha V.O., Tovar L.P., 2020, Pyrolysis of Humins Obtained from Acid-catalyzed Depolymerization of Rice Husk Cellulose: Model-free Approach to Non-isothermal Kinetics, Chemical Engineering Transactions, 80, 211-216 DOI:10.3303/CET2080036

economy is, therefore, categorical to add greater value to new products and to the whole integrated industrial unit through the production of synthesis gas. For the use of HUs as a material for synthesis gas production, studies and thermal analysis are required using thermogravimetric analyzers. The HUs, thus, undergo a pyrolysis process, where they are subjected to temperatures of 15°C until reaching the maximum temperature of 900°C. Therefore, this work investigates the value of the by-products obtained during the production of levulinic acid (LA), by means of the kinetic analysis of the pyrolysis of HUs obtained during the rice husk biorefining (agro-industrial waste) to modulate the concept of the new generation of biorefineries as a driver of an emerging bio-industry and an integrated platform based bio-economy.

2. Materials and method

The rice husk was provided by the Irmãos Pillon company (a rice industry from Santa Maria, RS, Brazil) and dried in the open until obtaining 10.5% of moisture content.
In Figure 1 it is possible to visualize the process of primary and secondary biorefining for producing levulinic acid, and the consequent production of HUs.

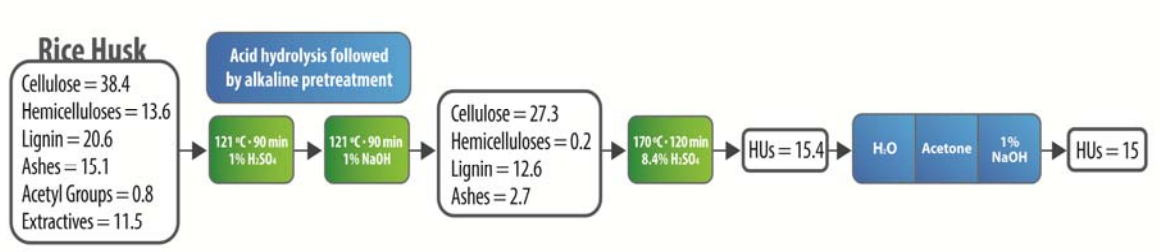

Figure 1: Generic flowchart of the HUs formation process during the primary and secondary biorefining of rice husk

2.1 Thermogravimetric analyzes

Thermogravimetric analyzes (TGA) and the first derivative of the TGA curve (the DTG curve) were obtained using a thermogravimetric analyzer "*Instrument TGA Q5000".* An inert atmosphere for pyrolysis was simulated by purging 50 mL·min^{-1} of nitrogen gas. In a previous study (results not discussed in this work) it was evidenced that between 1.5 and 2.5 mg of material there was no significant variation in the thermal degradation profile of the HUs at a certain heating rate (20 °C·min^{-1} and 40 °C·min^{-1}). Then, approximately 2.0 mg of HUs (with a particle size ranged from 1 to 10 µm) were loaded for analysis in a platinum crucible. The furnace was heated at a rate of 10 °C·min^{-1} until reaching the temperature of 105°C and remained in it for 10 minutes in order to ensure that the analyzes would begin with dry HU samples. After so, the samples were subjected to different heating rates: 10, 20, 30 and 40 °C·min^{-1} until reaching the maximum temperature of 900°C.

2.2 Kinetic analysis from thermogravimetric curves

From the thermogravimetric data were determined and investigated the kinetic parameters of the thermal decomposition of HUs using a non-isothermal model-free method.
It is believed that the thermal degradation of HUs involves several simultaneous reactions, since they are composed of heterogeneous materials, being difficult the detailing of each reaction that is part of this process.
The Global Reaction Mechanism (GRM) corresponds to a stage of decomposition of biochar material and volatile material (both condensable and non-condensable), as shown in Figure 2.

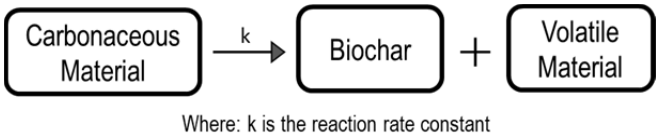

Figure 2: Pyrolysis reaction for GRM

Thus, when considering an initial approach, the GRM model can preliminarily describe the decomposition of HUs. The global kinetics of the thermal degradation reaction may be expressed by Equations 1 and 2:

$$\frac{d\alpha}{dt} = k(T)\, f(\alpha) \quad (1)$$

$$\alpha = \frac{m_0 - m_t}{m_0 - m_f} \quad (2)$$

Where *t* is the reaction time; *α* is the degree of conversion; m_0 is the initial mass of the sample; m_t is the mass of the sample at time t; m_f is the mass of the sample at the end of the reaction.
Assuming, then, that the reactions are parallel and independent, Equation 1 can be rewritten by putting the reaction rate as a function of temperature.

$$\frac{d\alpha}{dt} = k\left[f(\alpha)\right] = \left[A\exp\left(\frac{-E_a}{RT}\right)\right]\left[f(\alpha)\right] \quad (3)$$

where, E_α is the apparent activation energy ($J \cdot mol^{-1}$); *R* is the constant of the gases ($J \cdot mol^{-1} \cdot K^{-1}$); *A* is the pre-exponential factor (min^{-1}); *T* is absolute temperature (K).
For thermal degradation processes, a constant heating rate β is admitted. Therefore, it is possible to formulate the reaction rates as a function of temperature (Equation 4).

$$\frac{d\alpha}{dT} = \frac{A}{\beta}\exp\left(\frac{-E_a}{RT}\right)\left[f(\alpha)\right] \quad (4)$$

2.3 Non-isothermal model-Free for determining kinetic parameters

The model-free method approached in this work is part of a large group of methods, where E_α and *A* are estimated for a specific conversion α_i. For the Kissinger Method, it was determined that the kinetic parameters can be estimated at their maximum reaction rate.
Ghadikolaei et al. (2017) propose that, for Kissinger Method, the energy activation may be estimated using Equation 5.

$$\ln\left(\frac{\beta}{T_m^2}\right) = -\frac{E_\alpha}{RT_m} + \ln\left(\frac{-ARf'(\alpha)}{E_\alpha}\right) \quad (5)$$

When plotting the graph of $\ln\left(\frac{\beta}{T_m^2}\right)$ vs $\frac{1}{T_m}$ the activation energy was calculated from the slope of the line and the pre-exponential factor will be the value where the graph intercepts the y-axis (Ghadikolaei et al., 2017).

2.4 Estimations of thermodynamic parameters

Next, with E_a and *A* already obtained, the enthalpy variation (*ΔH*), Gibbs free energy (*ΔG*) and entropy variation (*ΔS*) were calculated from Equations 6-8, respectively, in order to define and characterize the HUs thermal decomposition mechanism (Yuan et al., 2017).

$$\Delta H = E_a - RT_\alpha \quad (6)$$

$$\Delta G = E_a + RT_m \ln\left(\frac{K_B T_m}{hA_i}\right) \quad (7)$$

$$\Delta S = \frac{\Delta H - \Delta G}{T_m} \quad (8)$$

where: K_b = Boltzmann constant (1.381×10^{-23} $J \cdot K^{-1}$), *h* is Planck constant (6.626×10^{-34} J·s); T_m is the temperature at the maximum peak of the DTG curve and T_α = temperature at the "*α*" conversion.

3. Results and discussion

The normalized DTG and normalized mass (W) curves for different heating rates are shown in Figure 3a and 3b. The effects of increasing the temperature consequently reduce the formation of gaseous products. The normalized DTG curve can be divided into three regions (Figure 3a). The Region (I) in the temperature range between 15 °C until the beginning of the pyrolysis stage (about 135 °C) that represents the release of moisture. At this stage, the volatilized mass released correspond to 13% (Figure 3b). Region (II) is known as the active pyrolysis zone. Within the active pyrolysis region in the normalized DTG curves (Figure 3a), two

peaks of mass loss rate appear for HUs in which a loss of mass of almost 42% was observed (at 424.2 °C, 434.5 °C, 440.3 °C and 446.0 °C when considering the heating rates: 10, 20, 30 and 40 °C·min^{-1}, respectively). Then, the loss of mass in this region was independent of the heating rates analyzed. After 600 °C, in the Region (III) or passive pyrolysis region the conversion rate is relatively lower reporting a mass loss dependent on the heating rate corresponding to the decomposition of retained carbonaceous materials in the coal residue. The final residue at 900 °C was 7%, 20%, 32% and 35% at 10, 20, 30 and 40 °C·min^{-1}, respectively (Figure 3b). The effect of increasing the heating rate defines a characteristic behavior of increasing the conversion rate. On the other hand, the shift of the peaks laterally towards higher temperatures when the heating rate was increased from 10 to 40 °C·min^{-1} was up to 22.9 K (in active pyrolysis - peak 1) and 21.8 K for (in active pyrolysis – peak 2), respectively, which indicates that pyrolysis did not find an impact on the heating rate due to the slow heat transfer (Pecha et al., 2019) within the carbonaceous fraction.

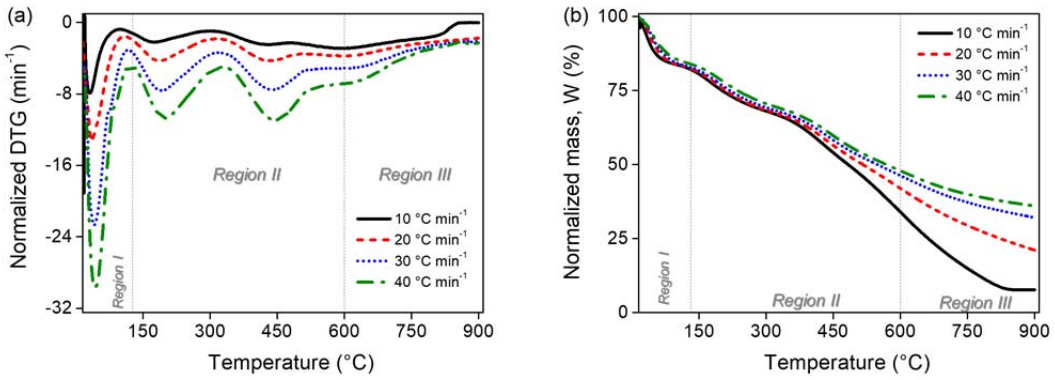

Figure 3: Thermogravimetric analyzes of HUs. (a) First derivative of the TGA curve (the DTG curve); (b) Normalized mass curve

3.1 Estimation of kinetic parameters

From the collected data, in Figure 4 the plots of Kissinger Method are plotted. Thus, E_α and A are estimated from the slope of the regression line and the y-axis intercept, respectively. Analyzing Table 1, the values of R^2 are 0.999 for both peaks, indicating that the estimated E_α values for the Kissinger method are reliable.

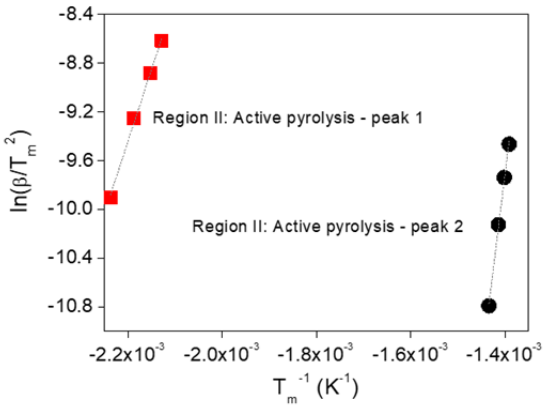

Figure 4: Linear regressions using the Kissinger Method

Ruksathamcharoen et al. (2019) analyzed hydrochars that underwent hydrothermal treatments. For the Power Law Model, E_α values reported by them, for stage 2 of the process, were of 75.81 kJ·mol^{-1} for the HTW-180 sample, and of 76.79 kJ·mol^{-1} for the HTW-200 one. These results are similar to those found in peak 1 (Region II-active pyrolysis) of the HUs of this work (97.838 kJ·mol^{-1}). For the Diffusion Model, the E_α reported values for the stage 2 of the process were of 132.59 kJ·mol^{-1} for the HTW-180 sample, and of 135.33 kJ·mol^{-1} for the HTW-200 sample. Another study that may be cited is the one of Yao et al. (2016), where hydrochars and waste of paper resulting from paper industries were analyzed. The E_α for stages 1, 2 and 3 of the process studied was mentioned at intervals, respectively, of 34.2-173.0 kJ mol^{-1}, 160.5-207.2 kJ mol^{-1} and 186.8-278.9

kJ mol^{-1} for different percentages of hydrochars. These results are also similar to those found in peak 2 of the HUs of this work (260,2 kJ·mol^{-1}). According to Balart et al. (2019), when the Kissinger Method is used, it must be assumed that f(α) is not altered with the conversion, and trusted values of E_α may be estimated if the conversion α_m, does not significantly change with the variation of the heating rate β. Observing Table 1, it is noted that in the two peaks reported for the region II-active pyrolysis, the variation of α_m is small, indicating a variation of 0.238 (rate of 10°C·min^{-1}) to 0.331 (rate of 40°C·min^{-1}) for peak 1 of HUs; of 0.462 (rate of 10°C·min^{-1}) to 0.622 (rate of 40°C·min^{-1}) for peak 2 of HUs. Therefore, once again, the viability of the estimated E_α values is indicated.

Regarding the analysis of the pre-exponential factor, the values are estimated and the natural logarithm for each *f(α)* kinetic function valid in this study is calculated (Table 1). For Maia and de Morais (2016), lower values of *A* are linked to lower values of E_α, meaning easier and faster degradation. Thus, the active pyrolysis of the HUs sample at peak 1 is faster and easier than at peak 2 in the region II-active pyrolysis.

3.2 Estimation of thermodynamic parameters

The thermodynamic parameters, ΔH, ΔG and ΔS, were calculated and reported in Table 1. Positive values of ΔH for each peak temperature in the region II-active pyrolysis reveal that the thermal degradation/pyrolysis of these HUs are endothermic reactions, referring to the need for an external heat source for the reaction to happen (Chen et al., 2017). It is clearly observed that in the thermal degradation defined by peak 2 in the region II-active pyrolysis ($\Delta H \approx 254$ kJ·mol^{-1}) demands much more heat than thermal degradation defined by peak 1 of HUs ($\Delta H \approx 94$ kJ·mol^{-1}). Parameter ΔS is a state function of the reaction system, representing the degree of disorder of this system (Yuan et al., 2017). Negative results for the entropy variation indicate that the disorder of products formed after the breaking of bonds is smaller than the disorder of the initial reagents. The ΔS ranges from -184.8 J·mol^{-1}·K^{-1} to -213.4 J·mol^{-1}·K^{-1} for peak 1 in the region II-active pyrolysis and from -175.7 J·mol^{-1}·K^{1} to -192.0 J·mol^{-1}·K^{-1} for peak 2 in the region II-active pyrolysis. According to Maia and de Morais (2016), low values of ΔS mean that the material went through some kind of degradation process, becoming near to its thermodynamic equilibrium state. In these cases, the sample has little reactivity and, as a result, the time for the formation of the activated complex is greater.

Parameter ΔG refers to the increase of the total energy of the system in favor of the reagents and the formation of the activated complex. It is known that high values of ΔG indicate low reaction favorability, thus, when analyzing Table 1 it is found that the thermal decomposition of HUs in peak 2 in the region II-active pyrolysis components is more favorable. In general, ΔG values raise with the increase of the heating rate.

Table 1: Peak properties of the HUs obtained for all heating rates (10, 20, 30 and 40 ° C·min^{-1}) and estimated values for E_α, and A using the adjusted R^2 Kissinger Method.

Parameters		f(α)[a]	Region II-active pyrolysis							
			Peak 1				Peak 2			
Heating rate, β (°C·min^{-1})			10	20	30	40	10	20	30	40
Peak temperature, T_m (°C)			173.4	184.2	191.2	196.3	424.2	434.5	440.3	446.0
Conversion at T_m, α_m (-)			0.238	0.282	0.323	0.331	0.462	0.529	0.600	0.622
Kinetics	E_α (kJ·mol^{-1})		97.8				260.2			
	ln A (min^{-1})	O1	12.2	12.2	12.2	12.2	13.9	13.9	13.9	13.9
		R2	12.7	12.7	12.7	12.7	14.3	14.2	14.1	14.1
		D2	9.3	9.6	9.9	9.9	12.3	12.6	12.8	12.9
		A1	12.2	12.2	12.2	12.2	13.9	13.9	13.9	13.9
	R^2		0.999				0.999			
Thermodynamics	ΔH (kJ·mol^{-1})		94.1	94.0	94.0	93.9	254.4	254.3	254.3	254.2
	ΔG (kJ·mol^{-1})	O1	178.8	180.7	182.2	183.1	379.2	381.0	382.1	383.0
		R2	176.7	178.7	180.2	181.2	377.0	379.1	380.7	381.8
		D2	189.5	190.4	190.8	191.8	388.3	388.7	388.6	389.2
		A1	178.8	180.7	182.2	183.1	379.2	381.0	382.1	383.0
	ΔS (J·mol^{-1}·K^{-1})	O1	-189.4	-189.6	-189.8	-189.8	-178.9	-179.0	-179.1	-179.2
		R2	-184.8	-185.2	-185.6	-185.7	-175.7	-176.4	-177.2	-177.5
		D2	-213.4	-210.7	-208.5	-208.3	-192.0	-190.0	-188.2	-187.7
		A1	-189.4	-189.6	-189.8	-189.8	-178.9	-179.0	-179.1	-179.2

[a] Mathematical expressions reported in Cai et al. (2018)

As shown in Table 1, the ΔG values in the temperature range of the analyzed peaks are positive, and the ones of ΔS are negative, so the thermal degradation processes of the samples at all heating rates are non-spontaneous at the temperatures in which they were submitted.

HUs are biopolymers formed unintentionally during the process of obtaining LA through hydrolytic sugars reactions (Lopes et al., 2017). As a result, studies are made aiming to expand the knowledge about HUs helping in the viability of this material. Its great potential is the production of synthesis gas and commodities

from the pyrolysis process, because, according to van Zandvoort et al. (2015), studies indicate that HUs are strong heat sources when undergoing this process or gasification. Therefore, HUs should be valued in the concept of bio-refinery due to different formation pathways and chemical structures.

4. Conclusions

The decomposition of the material into biochar and volatile material by the thermogravimetric profiles suggest the presence of parallel and independent reactions, where the decomposition of the main components of the carbonaceous material in a given temperature range is equivalent to the sum of the conversion rates obtained in the pyrolisys reaction of each one. The prelimanry kinetic analysis for HUs, allowed to estimate the E_α values at the region II-active pyrolysis equal to 97.8 (peak 1) and 260.2 $kJ \cdot mol^{-1}$ (peak 2), respectively. Positive ΔH values of the samples reveal that the reaction of thermal degradation of these HUs is endothermic. Evaluating the spontaneity of this reaction, positive ΔG and negative ΔS values show that they are non-spontaneous processes. An outlook investigating the suitability of different thermal degradation models as for example the 'Distribution of Activation Energies Model', DAEM is required to re-estimate the kinetics parameters and to describe the conversion rate curves.

Acknowledgments

This work was supported by National Council for Scientific and Technological Development - CNPq [Public investment by Universal Call MCTIC/CNPq n.º 28/2018 and grant number 408149/2018-3] and São Paulo Research Foundation - FAPESP [grant numbers 2015/20630-4].

References

Agarwal S., Van Es D. Heeres H.J., 2017, Catalytic Pyrolysis of Recalcitrant, Insoluble Humin Byproducts from C6 Sugar Biorefineries, Journal of Analytical and Applied Pyrolysis, 123, 134-143.

Balart R., Garcia-Sanoguera D., Quiles-Carrillo L., Montanes N. Torres-Giner S., 2019, Kinetic Analysis of the Thermal Degradation of Recycled Acrylonitrile-butadiene-styrene by Non-isothermal Thermogravimetry, Polymers (Basel), 11, 281.

Cai J., Xu D., Dong Z., Yu X., Yang Y., Banks S.W. Bridgwater A.V., 2018, Processing Thermogravimetric Analysis Data for Isoconversional Kinetic Analysis of Lignocellulosic Biomass Pyrolysis: Case Study of Corn Stalk, Renewable and Sustainable Energy Reviews, 82, 2705-2715.

Chen J., Wang Y., Lang X., Ren X.E. Fan S., 2017, Evaluation of Agricultural Residues Pyrolysis Under Non-Isothermal Conditions: Thermal Behaviors, Kinetics, and Thermodynamics, Bioresource Technology, 241, 340-348.

Ghadikolaei S.S., Omrani A. Ehsani M., 2017, Non-Isothermal Degradation Kinetics of Ethylene-Vinyl Acetate Copolymer Nanocomposite Reinforced with Modified Bacterial Cellulose Nanofibers Using Advanced Isoconversional and Master Plot Analyses, Thermochimica Acta, 655, 87-93.

Hayes M.H.B., Mylotte R. Swift R.S. 2017. Chapter Two - Humin: Its Composition and Importance in Soil Organic Matter. In: SPARKS, D. L. (ed.) Advances in Agronomy. Academic Press.

Leal Silva J.F., Maciel Filho R. Wolf Maciel M.R., 2018, Comparison of Extraction Solvents in the Recovery of Levulinic Acid from Biomass Hydrolysate using a Group Contribution Method, Chemical Engineering Transactions, 69, 373-378.

Lopes E., Dominces K., Lopes M., Tovar L. Maciel Filho R., 2017, A Green Chemical Production: Obtaining Levulinic Acid from Pretreated Sugarcane Bagasse, Chemical Engineering Transactions, 57, 145-150.

Maia A.a.D. De Morais L.C., 2016, Kinetic Parameters of Red Pepper Waste as Biomass to Solid Biofuel, Bioresource Technology, 204, 157-163.

Pecha M.B., Arbelaez J.I.M., Garcia-Perez M., Chejne F. Ciesielski P.N., 2019, Progress in Understanding the Four Dominant Intra-particle Phenomena of Lignocellulose Pyrolysis: Chemical Reactions, Heat Transfer, Mass Transfer, and Phase Change, Green Chemistry, 21, 2868-2898

Ruksathamcharoen S., Chuenyam T., Ajiwibowo M.W. Yoshikawa K., 2019, Thermogravimetric Analysis of Combustion Characteristics and Kinetics of Hydrothermally Treated and Washed Empty Fruit Bunch, Biofuels, 1-10.

Sasson A. Malpica C., 2018, Bioeconomy in Latin America, New Biotechnology, 40, 40-45.

Van Zandvoort I., Koers E.J., Weingarth M., Bruijnincx P.C.A., Baldus M. Weckhuysen B.M., 2015, Structural Characterization of 13C-Enriched Humins and Alkali-treated 13C Humins by 2D Solid-State NMR, Green Chemistry, 17, 4383-4392.

Yao Z., Ma X., Wu Z. Yao T. 2017. TGA–FTIR Analysis of Co-pyrolysis Characteristics of Hydrochar and Paper Sludge, Journal of Analytial and Applied Pyrolysis, 123, 40-48.

Yuan X., He T., Cao H. Yuan Q., 2017, Cattle Manure Pyrolysis Process: Kinetic and Thermodynamic Analysis with Isoconversional Methods, Renewable Energy, 107, 489-496.